

Evidence for field induced proximity type behavior in based ferromagnetic nanofluid

S. Sergeenkov, C. Stan, C. P. Cristescu, M. Balasoiu, N. S. Perov & C. Furtado

To cite this article: S. Sergeenkov, C. Stan, C. P. Cristescu, M. Balasoiu, N. S. Perov & C. Furtado (2017) Evidence for field induced proximity type behavior in based ferromagnetic nanofluid, *Philosophical Magazine Letters*, 97:7, 287-293, DOI: [10.1080/09500839.2017.1343959](https://doi.org/10.1080/09500839.2017.1343959)

To link to this article: <http://dx.doi.org/10.1080/09500839.2017.1343959>



Published online: 28 Jun 2017.



Submit your article to this journal [↗](#)



Article views: 6



View related articles [↗](#)



View Crossmark data [↗](#)



Evidence for field induced proximity type behavior in CoFe_2O_4 based ferromagnetic nanofluid

S. Sergeenkov^a, C. Stan^b, C. P. Cristescu^b, M. Balasoiu^{c,d}, N. S. Perov^e and C. Furtado^a

^aDepartment of Physics, Universidade Federal da Paraíba, João Pessoa, Brazil; ^bFaculty of Applied Physics, Department of Physics, Politehnica University of Bucharest, Bucharest, Romania; ^cJoint Institute for Nuclear Research, Dubna, Russia; ^dHoria Hulubei National Institute of Physics and Engineering, Bucharest, Romania; ^eFaculty of Physics, Lomonosov Moscow State University, Moscow, Russia

ABSTRACT

We report some unusual magnetic properties observed in CoFe_2O_4 based ferrofluid (with an average particle size of $D = 6$ nm). More precisely, in addition to the low-field ferromagnetic (FM) phase transition with an intrinsic Curie temperature $T_{Cb} = 350$ K, a second phase transition with an extrinsic Curie temperature $T_{Cw} = 266$ K emerges at higher (saturating) magnetic field. The transitions meet at the crossover point $T_{Cr} = 210$ K. The origin of the second transition is attributed to magnetic field induced proximity type interaction between FM particles through non-FM layers.

ARTICLE HISTORY

Received 4 May 2017
Accepted 12 June 2017

KEYWORDS

Ferrofluids; magnetic phase transitions; crossover

1. Introduction

Due to a large scale applicability, the nanostructured materials continue to attract considerable attention. Of special importance are the stable colloidal dispersions of ferromagnetic (FM) nanoparticles [1–5] which are also of interest both for experimental and theoretical studies related to the influence of different size effects on their structural and magnetic properties [6–10]. In particular, it was found [9,10] that the so-called finite temperature size effects can significantly reduce the amount of the ordered phase and the corresponding value of the Curie temperature. A high coercivity at room temperature, moderate saturation magnetization and good catalytic properties made cobalt ferrite (CoFe_2O_4) nanoparticles not only an ideal material for high density storage devices, photomagnetic applications, and molecular agents in magnetic resonance imaging but also proved them one of the most popular ingredients of ferrofluids [11–14]. It is now well established that the overall behavior of FM fluids is determined by a competition between their intrinsic (intraparticle) and extrinsic (interparticle) properties. However, a separate study of these two contributions still remains a challenging problem. On the other hand, it should be pointed out that despite the fact that ferrofluids are based on such a strong FM material as CoFe_2O_4 (with the Curie temperature as much as $T_C = 793$ K), their magnetic response is mistakenly treated within the Langevin model of paramagnetism (PM) which considers the magnetic fluid as a system composed by non-interacting spheres with a permanent

dipolar magnetic moment. So, when an external magnetic field is applied, the magnetic dipole moment of each nanoparticle experiences a torque which makes it rotate around the direction of the field. Therefore, the macroscopic magnetization within the Langevin scenario is the result of the combined action of magnetic moments orientation induced by the external field and the perturbation produced by the disordered Brownian motion (thermally activated diffusion) [6,11–13]. Needless to say that within this approach the most interesting feature of ferrofluids (related to the ordering of the FM particles below the corresponding Curie temperatures) is completely missing from the picture. In this regard, it is imperative to mention earlier theoretical attempts to model phase behavior of the ferrofluid based on the Curie–Weiss (rather than Langevin) concept by taking into account realistic interactions between FM particles within the fluid [15–17].

To properly address this important issue, in this Letter we present our latest results on the magnetic field and temperature behavior of CoFe_2O_4 based ferrofluids. We found that in addition to the major low-field phase transition (with the Curie temperature $T_{Cb} = 350$ K), a second phase transition (with the Curie temperature $T_{Cw} = 266$ K) is developing at higher (saturating) magnetic field. The origin of the second (extrinsic) transition is attributed to manifestation of strong field induced proximity type processes between the nearest particles in the ferrofluid.

2. Samples characterization and magnetic measurements

Samples of CoFe_2O_4 ferrofluid nanoparticles coated with a double layer of dodecylbenzenesulphonic acid (DBS) and dispersed in double distilled water were synthesized by chemical co-precipitation method presented in [11–13]. The structural characterization of our samples was performed by transmission electron microscopy (TEM) and small angle neutron scattering (SANS). The analysis of TEM images and SANS spectra confirmed [18] the presence of well-defined FM nanoparticles (with an average diameter of $D = 6$ nm) separated by non-FM layers (with an average thickness of $t = 3.5$ nm). Magnetic measurements were carried out on a LakeShore N7400 vibrating sample magnetometer in the temperature interval $110\text{K} \leq T \leq 350$ K. Figure 1 shows typical M – H curves (taken at $T = 350$ K) for low and high magnetic field regions. Notice that low-field hysteresis is quite strong (with coercive magnetic field $H_C = 0.2$ kOe).

3. Results and discussion

Figure 2 presents the dependence of the normalized magnetization $M(T)/M(T_p)$ on the reduced temperature T/T_{Cb} after subtraction of the paramagnetic contribution. Here, $M(T_p) = 0.29$ G with $T_p = 110$ K. More specifically, Figure 2a shows the temperature behavior of $M(T)$ under the low magnetic field $H = 0.4$ kOe. Likewise, Figure 2b presents the temperature dependence of magnetization $M(T)$ taken under the higher magnetic field $H = 16$ kOe with $T_p = 110$ K and $M(T_p) = 0.78$ G. As we can see, in this case $M(T)$ exhibits more interesting behavior. Namely, in addition to the major phase transition at $T_{Cb} = 350$ K, a second FM transition is emerging at $T_{Cw} = 266$ K. The inflection point at $T_{cr} = 210$ K indicates a clear-cut crossover between the two transitions. Similar crossover takes place in room-temperature nanogranular FM graphite [10] and in arrays of quantum dots [19]. Turning to the analysis of the obtained results, let us begin with

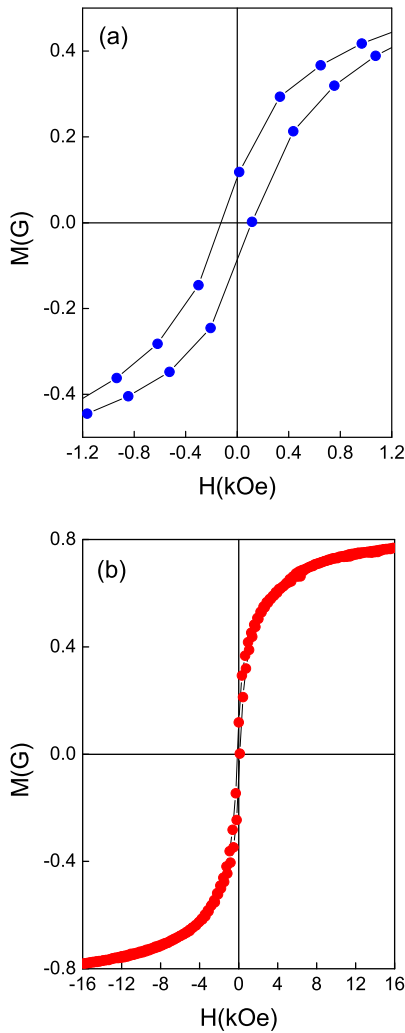


Figure 1. M - H curves taken at the highest temperature ($T = 350$ K) for low (a) and high (b) magnetic field regions.

the low-field magnetization. We were able to successfully fit the data using the following explicit expression for the single particle (intrinsic) magnetization:

$$M_b(T) = M_{sb} \tanh \left[\left(\frac{T_{Cb}}{T} \right)^4 - 1 \right] \quad (1)$$

which presents approximate solution of the Curie-Weiss mean-field equation for FM magnetization valid for all temperatures [4,5,9,10]. The solid line in Figure 2a is the best fit according to Equation (1) with $T_{Cb} = 350$ K and $M_{sb} = 0.25$ G. Notice that, according to Figure 1a, the value of M_{sb} well correlates with $M(H = 0.4$ kOe).

As far as the high-field magnetization is concerned, it is quite natural to assume that in addition to intrinsic contribution $M(T) = M_b(T)$ (given by Equation (1)) above

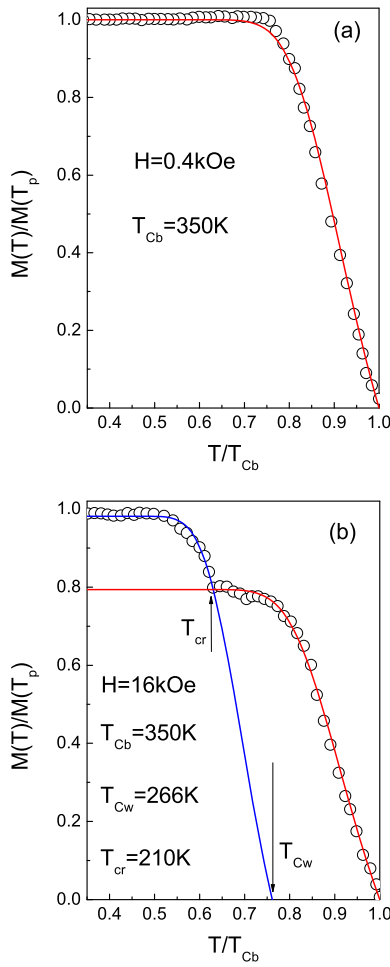


Figure 2. The dependence of the normalized magnetization $M(T)/M(T_p)$ on the reduced temperature T/T_{Cb} taken at low (a) and high (b) magnetic field. The solid lines are the best fits according to Equations (1)–(3).

the crossover point T_{cr} , the observed temperature behavior below T_{cr} can be attributed to manifestation of the field induced second phase transition (with the extrinsic Curie temperature $T_{Cw} = 266\text{K}$). More precisely, we were able to successfully fit all the high-field data using the following explicit expressions:

$$M_b(T) = M_{sb} \tanh \left[\left(\left(\frac{T_{Cb}}{T} \right)^4 - 1 \right) \right], \quad T > T_{cr} \quad (2)$$

and

$$M_w(T) = M_{sw} \tanh \left[\left(\left(\frac{T_{Cw}}{T} \right)^4 - 1 \right) \right], \quad T < T_{cr} \quad (3)$$

above and below the inflection point T_{cr} , respectively. The solid lines in Figure 2b present the best fits according to Equations (2) and (3) with $T_{Cb} = 350$ K, $T_{Cw} = 266$ K, $M_{sb} = 0.62$ G, and $M_{sw} = 0.78$ G.

To understand why the low-field magnetization does not exhibit a crossover, let us elucidate the origin of the second phase transition. Recall that in granular materials the interparticle (intergranular) contribution $M_w(T)$ is governed by the tunneling modified exchange interaction between the nearest particles with probability $\propto e^{-d/2\xi}$ where $d = 2t$ is the distance between neighboring particles ($t = 3.5$ nm is the thickness of the non-FM coating layer around FM nanoparticle in our ferrofluid) and $\xi = h/\sqrt{2mU}$ is a characteristic length with U being the potential barrier height, m an effective carrier mass and h the Plank constant. As a result, the interparticle (extrinsic) Curie temperature T_{Cw} can be related to the intraparticle (intrinsic) Curie temperature T_{Cb} as follows [10,19]

$$T_{Cw} = e^{-d/2\xi} T_{Cb} \quad (4)$$

Using the experimentally found values for T_{Cb} , T_{Cw} and d , from Equation (4) we obtain $\xi = 10$ nm for an estimate of the characteristic (coherence) length. It is important to keep in mind that the potential barrier U (and hence ξ) depends on applied magnetic field H . With a good enough accuracy, we can assume that $U(H) = U(0) - \mu H$ where μ is the total magnetic moment of the ferrofluid and a zero-field contribution $U(0)$ is dominated by the highest thermal energy which in our case is the bulk Curie temperature T_{Cb} , that is $U(0) \simeq k_B T_{Cb}$. At low magnetic fields (far from the saturation), $U(0) \gg \mu H$ and the potential barrier $U(H)$ is too high to provide an efficient tunneling between FM particles since in this case $\xi(H) \propto \frac{1}{\sqrt{U(H)}} \ll d$ leading to a strong reduction of the interparticle Curie temperature $T_{Cw} \ll T_{Cb}$ according to Equation (4). On the other hand, at high enough magnetic fields (near the saturation), $U(0) \simeq \mu H$ which results in a significant lowering of the barrier $U(H)$ and provides a strong interaction between the particles forming the nanofluid. In this case, $\xi(H) \simeq d$ leading to manifestation of the observed second phase transition at $T = T_{Cw}$. To better understand the difference between the low and high field situations, let us consider a particular example with $U(H_2) = 0.04U(H_1)$ where $H_1 = 0.4$ kOe and $H_2 = 16$ kOe. By definition, $\frac{\xi(H_1)}{\xi(H_2)} = \sqrt{\frac{U(H_2)}{U(H_1)}}$. So, in view of Equation (4) and recalling that $d = 7$ nm and $\xi(H_2) = 10$ nm, we obtain $\xi(H_1) \simeq 0.2\xi(H_2) \simeq 2$ nm and $T_{Cw}(H_1) \simeq 80$ K for low-field coherence length and the corresponding tunneling Curie temperature, respectively. This example demonstrates that at low fields (far below saturation) the interparticle contribution is shifted towards low temperatures making it more difficult to observe the proximity type effect in our samples.

Let us discuss now the origin of the crossover temperature T_{cr} . Notice that unlike the bulk temperature T_{Cb} , its weak-links-mediated counterpart T_{Cw} is strongly influenced by magnetic field. This becomes evident when we rewrite Equation (4) as follows, $T_{Cw}(H) = e^{-d/2\xi(H)} T_{Cb}$. According to Equations (2) and (3), $T_{cr}(H)$ is given by the solution of the equation $M_b(T_{cr}) = M_w(T_{cr})$ for a fixed value of $T_{Cw}(H)$. The result is presented in Figure 3 which depicts the dependence of the reduced crossover temperature $T_{cr}(H)/T_{Cb}$ on the ratio $T_{Cw}(H)/T_{Cb}$. As we can see, the value of the crossover temperature directly follows the value of the extrinsic Curie temperature, that is $T_{cr}(H) \propto T_{Cw}(H)$. Two relevant reference points, corresponding to $H = 0.4$ kOe and $H = 16$ kOe, are marked with arrows.

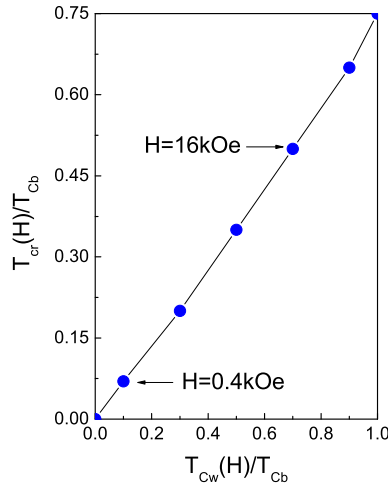


Figure 3. The dependence of the reduced crossover temperature $T_{cr}(H)/T_{Cb}$ on the ratio $T_{Cw}(H)/T_{Cb}$. The dots are the solutions of the equation $M_b(T_{cr}) = M_w(T_{cr})$.

And finally, an important comment is in order regarding the absolute value of the single particle Curie temperature $T_{Cb} = 350$ K. Recall [20] that the Curie temperature of the bulk CoFe_2O_4 crystal can reach as much as $T_C = 793$ K. This seeming discrepancy has to do with a pronounced size effect in nanoparticles. To quantify this statement, we can relate these two temperatures using the concept of the thermal de Broglie wavelength $\Lambda = h/\sqrt{mk_B T}$ which is responsible for finite temperature size effects in nanogranular materials [10]. More explicitly, one of such relationships between T_C and T_{Cb} reads:

$$T_{Cb} = \left(\frac{D}{D + \Lambda} \right) T_C \quad (5)$$

where D is the size (diameter) of the particle. When the size effects are negligible (that is when $D \gg \Lambda$), from Equation (5) we obtain $T_{Cb} \simeq T_C$. For the highest temperature in our study ($T = 350$ K), we have $\Lambda \simeq 8$ nm for an estimate of the de Broglie wavelength (assuming a free electron mass for m). Therefore, for nanoparticles with an average size of $D = 6$ nm (with $D \simeq \Lambda$) the size effects in our ferrofluid can not be neglected leading to a rather strong reduction of the bulk Curie temperature T_C . More precisely, given the above estimates, Equation (5) predicts $T_{Cb} = 0.44T_C \simeq 348$ K for the true Curie temperature of a single particle in our sample, in a rather good agreement with the observations.

4. Conclusions

In summary, the analysis of the high-temperature behavior of magnetization in CoFe_2O_4 based ferrofluid revealed the presence of two phase transitions. The first (major) transition takes place inside single particle. With increasing an applied magnetic field to the saturation level, a second transition starts to develop at lower temperature. Its origin is attributed to manifestation of rather strong proximity type effects between FM nanoparticles separated by non-FM layers.

Acknowledgements

The authors thank Dr L. Fetisov for realization of magnetic measurements.

Disclosure statement

No potential conflict of interest was reported by the authors.

Funding

The financial support through the grants of the Romanian Governmental Representative in the Joint Institute for Nuclear Research (JINR) and the UPB-JINR Cooperation Programme of scientific projects for the period 2016–2017 is acknowledged. This work was partially supported by Brazilian agencies CNPq, CAPES and FAPESQ [DCR-PB].

References

- [1] S.W. Charles, The preparation of magnetic fluids, in *Ferrofluids: Magnetically Controllable Fluids and their Applications*, S. Odenbach, ed., Lecture Notes in Physics, Springer-Verlag, Heidelberg, 2002, p. 3.
- [2] M.I. Shliomis, Ferrohydrodynamics: Retrospective and issues, in *Ferrofluids: Magnetically Controllable Fluids and their Applications*, S. Odenbach, ed., Lecture Notes in Physics, Springer-Verlag, Heidelberg, 2002, p. 85.
- [3] N.S. Souza, S. Sergeenkov, C. Speglich, V.A.G. Rivera, C.A. Cardoso, H. Pardo, A.W. Mombru, A.D. Rodrigues, O.F. de Lima and F.M. Araujo-Moreira, *Appl. Phys. Lett.* 95 (2009) p.233120.
- [4] N.S. Souza, A.D. Rodrigues, C.A. Cardoso, H. Pardo, R. Faccio, A.W. Mombru, J.C. Galzerani, O.F. de Lima, S. Sergeenkov and F.M. Araujo-Moreira, *Phys. Lett. A* 376 (2012) p.544.
- [5] N.S. Souza, S. Sergeenkov, A.D. Rodrigues, C.A. Cardoso, H. Pardo, R. Faccio, A.W. Mombru, J.C. Galzerani, O.F. de Lima and F.M. Araujo-Moreira, *J. Nanofluids* 1 (2012) p.143.
- [6] L. Vekas, M.V. Avdeev and D. Bica, Magnetic nanofluids: Synthesis and structure, in *Nanoscience and its Applications in Biomedicine*, D. Shi, ed., Springer Verlag, New York, 2009, p. 645.
- [7] X.H. Li, C.L. Xu, X.H. Han, L. Qiao, T. Wang and F.Sh. Li, *Nanoscale Res. Lett.* 5 (2010) p.1039.
- [8] C. Stan, C.P. Cristescu, M. Balasoiu, N. Perov, V.N. Duginov, T.N. Mamedov and L. Fetisov, *UPB Sci. Bull. A* 73 (2011) p.117.
- [9] S. Sergeenkov, N.S. Souza, C. Speglich, V.A.G. Rivera, C.A. Cardoso, H. Pardo, A.W. Mombru and F.M. Araujo-Moreira, *J. Phys.: Condens. Matter* 21 (2009) p.495303.
- [10] S. Sergeenkov, N.S. Souza, C. Speglich, V.A.G. Rivera, C.A. Cardoso, H. Pardo, A.W. Mombru and F.M. Araujo-Moreira, *J. Appl. Phys.* 106 (2009) p.116101.
- [11] D. Bica, *Rom. Rep. Phys.* 47 (1995) p.265.
- [12] M. Balasoiu, B. Grabcev and D. Bica, *Rom. Rep. Phys.* 47 (1995) p.319.
- [13] D. Bica, L. Vekas, M.V. Avdeev, O. Marinica, V. Socoliuc, M. Balasoiu and V.M. Garamus, *J. Mag. Mag. Mater.* 311 (2007) p.17.
- [14] A. Joseph and S. Mathew, *ChemPlusChem* 79 (2014) p.1382.
- [15] M. Ausloos, P. Clippe, J.M. Kowalski and A. Pekalski, *IEEE Trans. Magnetics* 16 (1980) p.233.
- [16] M. Ausloos, P. Clippe, J.M. Kowalski and A. Pekalski, *Phys. Rev. A* 22 (1980) p.2218.
- [17] M. Ausloos, P. Clippe, J.M. Kowalski, J. Pekalska and A. Pekalski, *Phys. Rev. A* 28 (1983) p.3080.
- [18] C. Stan, M. Balasoiu, A.I. Ivankov and C.P. Cristescu, *Rom. Rep. Phys.* 68 (2016) p.270.
- [19] S. Sergeenkov and M. Ausloos, *Phil. Mag. Lett.* 95 (2015) p.534.
- [20] C.D. Mee and E.D. Daniel, *Magnetic Recording Technology*, McGraw Hill, New York, 1996.